Boundary-Layer Meteorol
DOI 10.1007/s10546-012-9720-y

RESEARCH NOTE

On the Formation of an Elevated Nocturnal Inversion Layer in the Presence of a Low-Level Jet: A Case Study

Jakob Kutsher · Nitsa Haikin · Avi Sharon · Eyal Heifetz

Received: 16 April 2011 / Accepted: 13 March 2012

Abstract We report on observed nocturnal profiles, in which an inversion layer is located at the core of a low-level jet, bounded between two well-mixed layers. High-resolution vertical profiles were collected during a field campaign in a small plain in the Israeli desert (Negev), distant 100 km from the eastern shore of the Mediterranean Sea. During the evening hours, the synoptic flow, superposed on the late sea breeze, forms a low-level jet characterized by a maximum wind speed of 12 m s^{-1} at an altitude of 150 m above the ground. The strong wind shear at the jet maximum generates downward heat fluxes that act against the nocturnal ground cooling. As a result, the typical ground-based nocturnal inversion is "elevated" towards the jet centre, hence a typical early morning thermal profile is observed a few hours after sunset. Since the jet is advected into the region, its formation does not depend on the presence of a surface nocturnal inversion layer to decouple the jet from surface friction. On the contrary, here the advected low-level jet acts to hinder the formation of such an inversion. These unusual temperature and wind profiles are expected to affect near-ground dispersion processes.

Keywords Low-level jet · Nocturnal inversion · Stable boundary layer · Turbulent mixing

1 Introduction

Typically, in cloud-free and calm conditions, the daytime well-mixed boundary layer is transformed into a nocturnal inversion layer due to rapid radiative cooling (cf. Stull 1988). The strong stratification in the inversion layer acts to decouple the layer above from surface friction and as a result a low-level jet (LLJ) may be generated at the top

J. Kutsher (✉) · N. Haikin · E. Heifetz
The Department of Geophysical, Atmospheric and Planetary Sciences,
Tel-Aviv University, Ramat-Aviv, Tel Aviv, Israel
e-mail: yakovkut@tau.ac.il

A. Sharon
NRCN, P.O.B. 9001, Beer-Sheva, Israel

Published online: 01 April 2012

of the inversion layer. This mechanism was suggested originally by Blackadar (1957) and recently solved analytically by Shapiro and Fedorovich (2010). Under these conditions the turbulent mixing below the LLJ tends to be suppressed by the strong stratification.

On the other hand, LLJs can be formed by other mechanisms (such as baroclinic torque at the synoptic scale, fronts, land and sea breezes, as well as mountain and valley winds) and then become advected above a nocturnal stable boundary layer (SBL) (Stull 1988). When the LLJ is located lower than 300 m above the ground, it may induce a considerable amount of shear turbulence and non-zero turbulent fluxes into the SBL (Mahrt et al. 1979; Lenschow et al. 1988; Smedman et al. 1993, 1995, 1997; Mahrt and Vickers 2002; Banta et al. 2002).

Over the last decade, a joint effort has been made to characterize the shear above and beneath the LLJ maximum and the associated instabilities within the SBL (Banta et al. 2003, 2006; Cuxart and Jimenez 2007; Cuxart 2008; Banta 2008; Ohya et al. 2008). Nevertheless, as concluded by Cuxart (2008), ad hoc experiments are still required to study the mixing efficiency across the jet maximum and its effects on the SBL below and the free atmosphere above. In the current Note, we study several unusual nocturnal profiles obtained during a field campaign, in which the SBL is "lifted up" from the ground to the LLJ centre, apparently due to turbulent mixing.

2 The Field Campaign

During the summer of 2005, a boundary-layer sounding campaign was conducted in a semi-arid region located above a small plain in the Negev desert of Israel (location 4 on the map in Fig. 1a). The on-site experimental equipment included a high-resolution GPS-based radiosounding system with 1-Hz sampling frequency, providing a 3–4 m vertical resolution

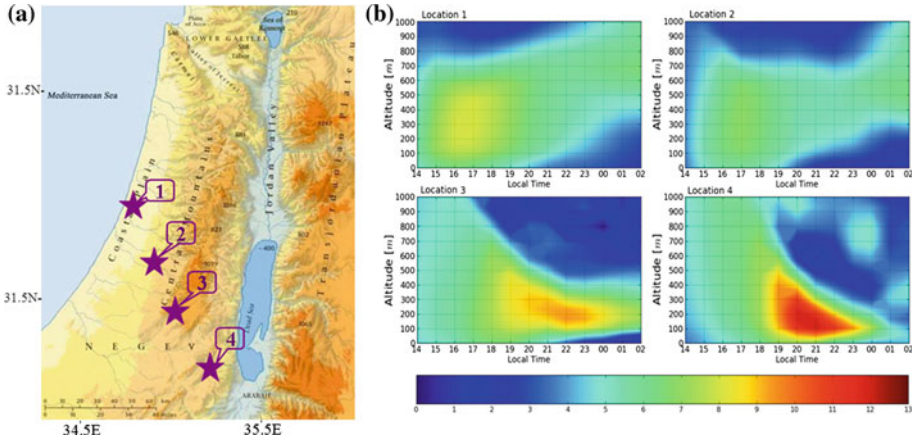

Fig. 1 **a** A regional eastern Mediterranean topography map indicating four selected locations along the inland flow trajectory (marked by *stars 1–4*). *Star 4* represents the campaign site. **b** Temporal-vertical cross-section of wind speed (m s^{-1}) obtained from a numerical mesoscale model above the four locations. Note that the wind speed increases while the flow penetrates inland and a LLJ is established above the campaign site, between 2000 and 2200 LT, about 150 m above ground level

(depending on vertical fluctuations) of wind and temperature profiles. Each sounding provides instantaneous wind-speed and temperature profiles with an accuracy at any level of 0.15 m s^{-1} and 0.5°C, respectively.

Overall, 50 soundings were taken on 15 active days (sampling the summer from early July to early September). Each day, at least three soundings were taken: afternoon (1400–1600 local time), late evening (2100–2300) and early morning (0300). Here and below, the time refers to the local time (LT), UTC +3.

3 Regional Synoptic Conditions

The Negev area is a semi-arid region and mostly cloud-free in summer, but it is only 100 km distant from the Mediterranean Sea and therefore is affected by the inland sea-breeze flow. The summer weather conditions over the eastern Mediterranean (hereafter EM) region are exceptionally persistent (Ziv et al. 2004). The lower levels are dominated by a low-pressure trough, also known as the 'Persian trough', which is an extension of the Indian monsoon system, and combined with upper-level subsidence (described in detail in Alpert et al. 1990, 2004; Bitan and Saaroni 1992; Saaroni and Ziv 2000). The trough is manifested by three essential modes (deep, moderate and shallow), according to the magnitude and the configuration of the horizontal pressure gradient at low levels (Dayan et al. 2002).

In the afternoon (between 1400 and 1700 LT) the sea breeze along the EM coast reaches its maximum intensity, superposed with the synoptic flow, and advects cool sea air inland (Dayan et al. 2002). The inland flow vector depends on the specific mode of the Persian trough: when the Persian trough is deep or moderate, the inland flow is towards east–south-east and does not reach the campaign site. However, when the Persian trough is shallow the flow is towards south–south-east, and may reach the site as a LLJ during the early hours of the night (Fig. 1b).

4 Composite Analysis

From 15 sampled summer days, only in three is the Persian trough mode deep or moderate (Fig. 2, upper row). As can be seen from the composite measured profiles on these three days, the diurnal cycle follows the expected quiescent scenario—after sunset a daytime well-mixed layer (just above a thin hyper-adiabatic surface layer) is cooled from below and the nocturnal surface inversion layer is established below the well-mixed layer (schematically shown in Fig. 3a). In contrast, in the other 12 sampled days (Fig. 2, lower row), the shallow Persian trough dominated and the composite profiles reveal a rather surprising scenario—the daytime well-mixed layer is cooled from below during the late evening but remains well-mixed as the LLJ reaches the site. Furthermore, an inversion layer is established above it at the LLJ centre (Fig. 3b).

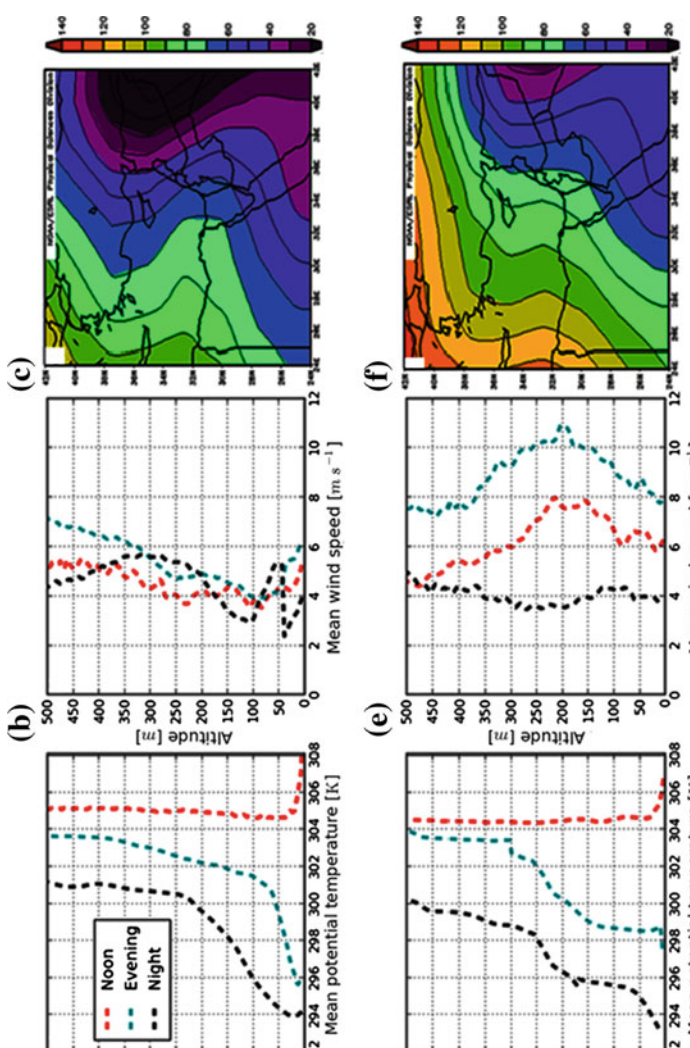

Fig. 2 Mean profiles of potential temperature and wind speed as measured at the campaign site, with a composite of 1,000-hPa geopotential height contours (NCEP-NCAR re-analysis archive; Kalnay et al. 1996). In the *upper row*, the composite is of the three cases in which the Persian trough was deep or moderate, and as a result the marine inland flow did not reach the site. In the *lower row*, the composite is of the 12 cases in which the Persian trough was shallow and consequently the inland flow formed a LLJ during the evening hours

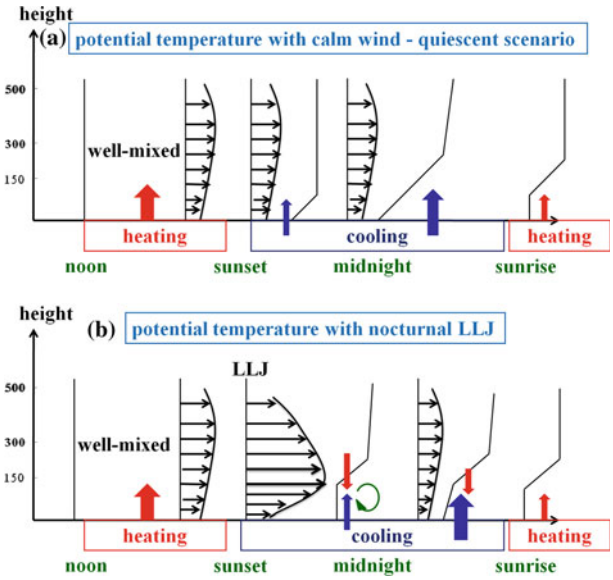

Fig. 3 Schematic illustration of the diurnal evolution of the potential-temperature and wind-speed profiles and the associated heat fluxes (positive and negative heat fluxes are presented as *red* and *blue arrows*, respectively): **a** in a quiescent scenario the daytime well-mixed layer is cooled from below after sunset, and the nocturnal surface inversion layer is established. In early morning the surface heating yields a thin surface mixed layer that is temporarily separated from the upper mixed layer by an aloft inversion. **b** In the presence of a nocturnal LLJ the shear induced turbulence at the jet maximum, generates downward heat flux that acts against the surface radiative cooling. As a result, a well-mixed surface boundary layer is generated, separated by an inversion layer from the mixed layer above it (as in the early morning profile). During the night, as the jet weakens and the radiative cooling increases, a surface inversion is established to match the elevated inversion from below

5 Case Study

In order to better understand the latter phenomena we focus on a single-day case study (September, 5), with a shallow Persian trough (Fig. 4). During that day, three soundings were taken, at 1800, 2100, 0300 LT, before, during and after the LLJ occurrence at the site, respectively. In addition, a mesoscale simulation was preformed to obtain the spatio-temporal evolution of the LLJ and to quantify the on-site heat fluxes.

The three-dimensional, non-hydrostatic Regional Atmospheric Modelling System (RAMS; Pielke et al. 1992) was employed with a 2.5-level turbulent closure, prognostic turbulent kinetic energy equation, and a diagnostic mixing length scale (Mellor and Yamada 1982). The grid configuration consisted of two-way nested grids with successive horizontal resolutions of 32, 8 and 2 km. The inner domain size is $116 \times 116\,\mathrm{km}^2$ (Fig. 5). The vertical grid consisted of 12 levels in the lowest 1 km above ground level, commencing with 50-m resolutions near ground. For lateral boundary conditions NCEP 1 degree global re-analysis data were used, every 6 h (Kalnay et al. 1996). The overall simulation period was 48 h. Simulation results for 1-min timesteps of wind, potential temperature and heat fluxes were used for the case study analysis.

Four sites along the flow path (towards the south–south-east) were chosen in order to study the spatial evolution of the LLJ from the coastal plain to the Negev campaign site (Fig. 1a). Temporal-vertical cross-sections of wind speed indicated that the flow was enhanced while

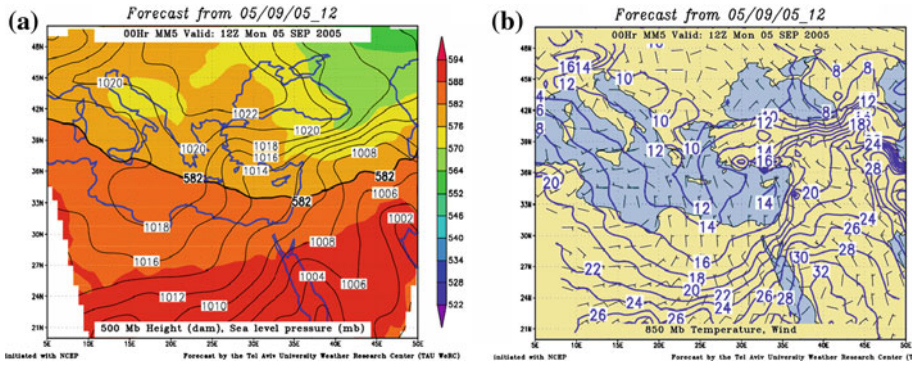

Fig. 4 Eastern Mediterranean synoptic characteristic weather charts at September 5, 2005: **a** Sea level pressure and 500-hPa level contours of the shallow Persian trough synoptic system. **b** Wind vectors and isotherms at the 850-hPa level. Note the south–south east direction over the inland area and the strong temperature gradient there. Both maps were obtained from the Weather Research Centre (TAU-WERC) and provided by ISA-MEIDA (http://nasa.proj.ac.il/)

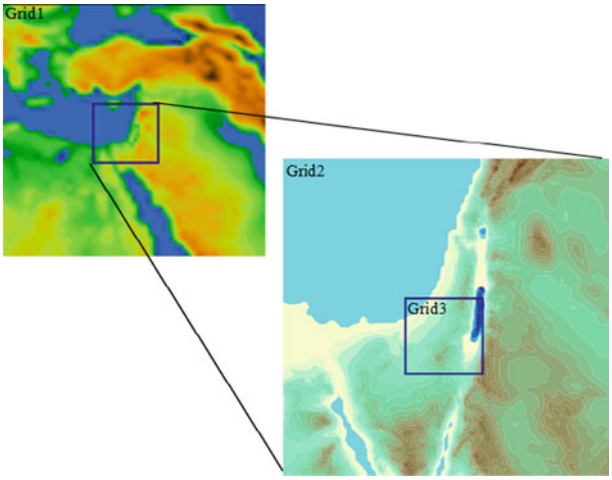

Fig. 5 Domains of the three nested grids used for the RAMS simulation with successive horizontal resolution of 32, 8 and 2 km (*grid 1, 2, 3* respectively)

penetrating deeper inland (Fig. 1b). Over the site, the LLJ was maximized in late evening (2000–2200 LT) with a wind-speed maximum of 12 m s^{-1} at about 150 m above ground level. This is consistent with the sea-breeze duration at the specific locations 1–4.

Profiles extracted from RAMS results were incorporated with the observed soundings (Fig. 6). The good agreement between the two provides confidence both in the measurements and the simulations. At 1800 LT (sunset), before the LLJ was detected, the boundary layer was well mixed as expected. When the LLJ was first observed above the site at 2000 LT, the temperature of the layer between the surface and the LLJ maximum decreased, however the layer remained remarkably well-mixed. Above it, an elevated nocturnal inversion was established bounded between the two well-mixed layers. A similar temperature profile was observed at the site, 1 h later (2100). Such a profile is typically expected in the early morning quiescent scenario when the nocturnal surface inversion layer is heated from below (Fig. 3a). RAMS simulated profiles indicated the existence of the elevated inversion until 2200 LT.

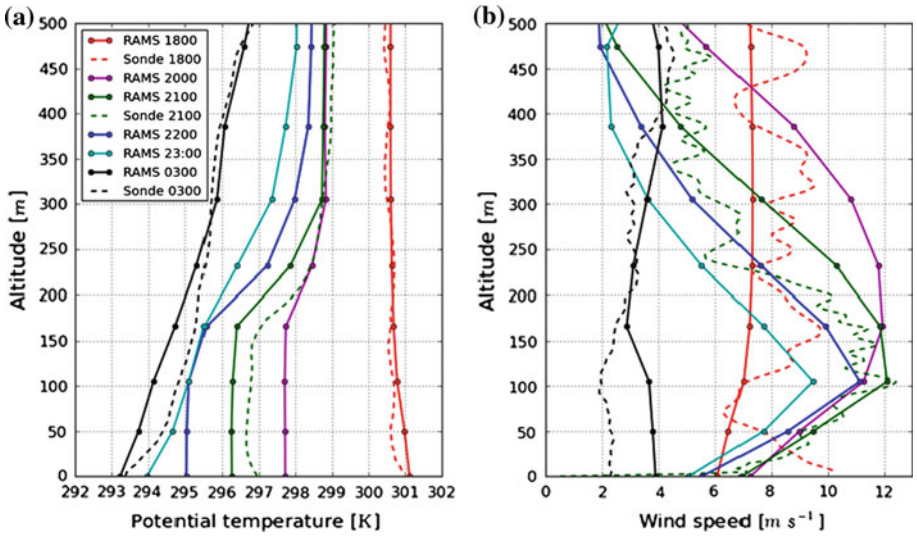

Fig. 6 Observation (*dashed line*) and simulation (*solid lines*) profiles of potential temperature (**a**) and wind speed (**b**) at the campaign site. The *dots* indicate the vertical resolution of the simulation

During the following hours, the temperature near the ground continued to decrease due to radiative cooling. By 0300 LT, the LLJ decayed and the common surface-based inversion was obtained and matched the elevated nocturnal inversion from below.

In order to understand why the layer below the LLJ maximum remains well-mixed we evaluated, from the RAMS simulation, the different terms contributing to the mean temperature tendency (Stull 1988):

$$\underbrace{\frac{\partial\overline{\theta}}{\partial t}}_{\mathrm{I}} = -\underbrace{\overline{u}\frac{\partial\overline{\theta}}{\partial x}}_{\Pi} - \underbrace{\frac{\partial(\overline{u'\theta'})}{\partial x}}_{\Pi\mathrm{I}} - \underbrace{\overline{w}\frac{\partial\overline{\theta}}{\partial z}}_{I\!V} - \underbrace{\frac{\partial(\overline{w'\theta'})}{\partial z}}_{V} + \underbrace{\overline{J}}_{V\mathrm{I}}, \tag{1}$$

where θ is the potential temperature, x is taken as the direction of the horizontal velocity u (pointing toward south–south east as the LLJ), z and w are the vertical direction and vertical velocity. Equation terms are described as follows: I—mean storage of heat; II—mean horizontal advection of heat; III—turbulent horizontal divergence of heat flux; IV—mean vertical advection of heat; V—turbulent vertical convergence of heat flux; and VI—longwave radiation divergence.

The horizontal wind component perpendicular to the LLJ is smaller by one order of magnitude than the wind component along the LLJ and found to contribute very little to the heat-flux budget. We used a time-averaging window of $T = 1$ h, where:

$$f = \overline{f} + f', \tag{2a}$$

$$\overline{f} = \frac{1}{T}\int_{t-\frac{T}{2}}^{t+\frac{T}{2}} f\,\mathrm{d}t \tag{2b}$$

Figure 7 presents the calculated profiles of Eq. 1 terms at 2100 LT (the time of the actual in-situ sounding). It is evident that the surface radiative cooling dominates the cooling below

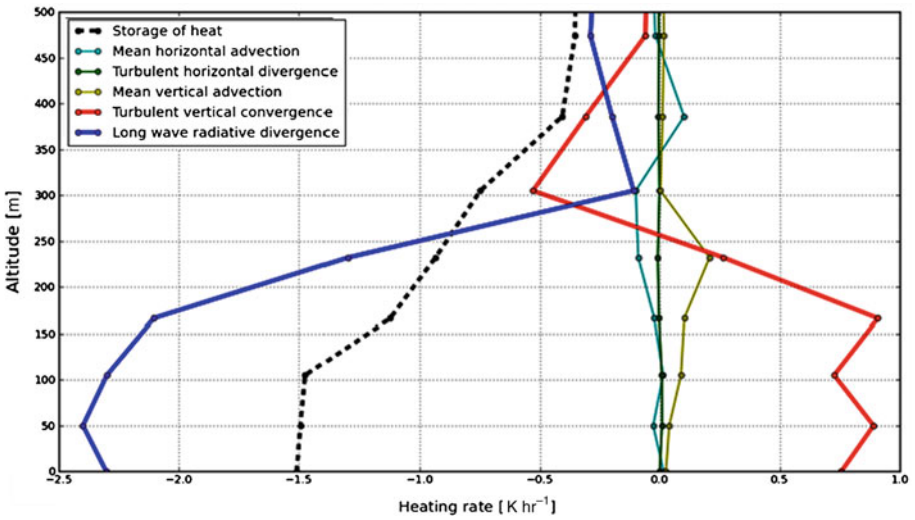

Fig. 7 Terms in Eq. 1, contributing to the potential temperature tendency at the site at 2100 LT (averaged between 2030 and 2130), calculated from the RAMS simulation at the campaign grid point. As in Fig. 6, the *dots* indicate the vertical resolution of the simulation

the LLJ maxima, whereas the turbulent vertical heat-flux convergence acts to warm the layer. Consequently, the temperature continues to decrease due to the overwhelming radiative cooling, although the layer becomes well-mixed. This is probably due to the turbulent mixing generated by the wind shear below the LLJ maximum (cf. the schematic illustration in Fig. 3b). All other terms of Eq. 1 contribute little to the heat budget near the surface, and the overall cooling rate up to 100 m is about 1.5 K h^{-1}. This agrees with the profiles shown in Fig. 6.

In contrast with the Blackadar scenario, here the well-mixed layer cannot "shield" the LLJ from surface friction (the bulk Richardson number is practically zero there). In addition, the LLJ decays as the sea-breeze front moves further toward the south–south east. Consequently, the turbulent mixing is suppressed and eventually, towards midnight, the nocturnal surface radiative inversion layer prevails and matches the elevated inversion layer from below.

6 Conclusions

In this Note we described observationally and numerically a nocturnal profile, in which the SBL is "lifted up" from the ground to the core of the LLJ, apparently due to turbulent mixing. As a result, a well-mixed surface layer is separated from an upper well-mixed layer by an elevated inversion at the jet maximum. This scenario is very different from the quiescent one, in which a surface inversion is generated below a well-mixed layer.

Although the suggested mechanism seems quite robust, it is the first time that this has been documented to the best of our knowledge. This might be because this mechanism is intrinsically transient: the LLJ generates a well-mixed layer below it, which in turn facilitates the suppression of the LLJ by surface friction. Furthermore, the campaign was performed in a season where the particular synoptic flow, superposed upon the sea breeze, is exceptionally persistent. In different regions, with much higher variability, it could be more difficult to document this phenomenon.

Such a profile is expected to alter the near-surface dispersion processes and in turn the air quality at the ground. Hence, it would be interesting to perform passive tracer dispersion experiments to evaluate the actual dispersion mixing processes under such conditions.

Acknowledgments The authors would like to thank Mr. Rony Neuman (NRCN) and Prof. Uri Dayan (HUJI) for useful discussions; NCEP Reanalysis data provided by the NOAA/OAR/ESRL PSD, Boulder, CO, USA, from their Web site at http://www.esrl.noaa.gov/psd/. The authors are also in debt to the anonymous reviewers for their valuable comments. E.H is grateful to the United States–Israel Binational Science Foundation (BSF) grant # 2008436.

References

Alpert P, Abramski R, Neeman BU (1990) The prevailing summer synoptic system in Israel subtropical high, not Persian trough. Israel J Earth Sci 39:93–102

Alpert P, Osetinsky I, Ziv B, Shafir H (2004) A new seasons' definition based on the classified daily synoptic systems, an example for the eastern Mediterranean. Int J Climatol 24:1001–1011

Banta RM (2008) Stable-boundary-layer regimes from the perspective of the low-level jet. Acta Geophys 56:58–87

Banta RM, Newsom RK, Lundquist JK, Pichugina YL, Coulter RL, Mahrt L (2002) Nocturnal low-level jet characteristics over Kansas during CASES-99. Boundary-Layer Meteorol 105:221–252

Banta RM, Pichugina YL, Newsom RK (2003) Relationship between low-level jet properties and turbulence kinetic energy in the nocturnal stable boundary layer. J Atmos Sci 60:2549–2555

Banta RM, Pichugina YL, Brewer WA (2006) Turbulent velocity-variance profiles in the stable boundary layer generated by a nocturnal low-level jet. J Atmos Sci 63:2700–2719

Bitan A, Saaroni H (1992) The horizontal and vertical extension of the Persian Gulf trough. Int J Climatol 12:733–747

Blackadar AK (1957) Boundary layer wind maxima and their significance for the growth of nocturnal inversions. Bull Am Meteorol Soc 38:283–290

Cuxart J (2008) Nocturnal basin low-level jets: an integrated study. Acta Geophys 56:100–113

Cuxart J, Jimenez MA (2007) Mixing processes in a nocturnal low-level jet: an LES study. J Atmos Sci 64:1666–1679

Dayan U, Lifshitz-Goldreich B, Pick K (2002) Spatial and structural variation of the atmospheric boundary layer during summer in Israel-profiler and rawinsonde measurements. J Appl Meteorol 41:447–457

Kalnay E et al (1996) The NCEP/NCAR 40-year reanalysis project. Bull Am Meteorol Soc 77:437–470

Lenschow DH et al (1988) The stably stratified boundary layer over the Great Plains. I. Mean and turbulent structure. Boundary-Layer Meteorol 42:95–121

Mahrt L, Vickers D (2002) Contrasting vertical structures of nocturnal boundary layers. Boundary-Layer Meteorol 105:351–363

Mahrt L, Heald RC, Lenschow DH, Stankov BB, Troen IB (1979) An observational study of the structure of the nocturnal boundary layer. Boundary-Layer Meteorol 17:247–264

Mellor GL, Yamada T (1982) Development of a turbulence closure model for geophysical fluid problems. Rev Geophys Space Phys 20:851–875

Ohya Y, Nakamura R, Uchida T (2008) Intermittent bursting of turbulence in a stable boundary layer with low-level jet. Boundary-Layer Meteorol 26:349–363

Pielke RA, Cotton WR, Tremback CJ, Lyons WA, Grasso LD, Nicholls ME, Moran MD, Wesley DA, Lee TJ, Copeland JH (1992) A comprehensive meteorological modeling system. Meteorol Atmos Phys 49:69–91

Saaroni H, Ziv B (2000) Summer rainfall in a Mediterranean climate—the case of Israel: climatological-dynamical analysis. Int J Climatol 20:191–209

Shapiro A, Fedorovich A (2010) Analytical description of a nocturnal low-level jet. Q J Roy Meteorol Soc 136:1255–1262

Smedman AS, Tjernström M, Högström U (1993) Analysis of the turbulence structure of a marine low-level jet. Boundary-Layer Meteorol 66:105–126

Smedman AS, Bergström H, Högström U (1995) Spectra, variances and length scales in a marine stable boundary layer dominated by a low-level jet. Boundary-Layer Meteorol 76:211–232

Smedman AS, Bergström H, Grisogono B (1997) Evolution of stable internal boundary layers over a cold sea. J Geophys Res 102:1091–1099

Stull RB (1988) An introduction to boundary layer meteorology. Kluwer, Dordrecht, 666 pp

Ziv B, Saaroni H, Alpert P (2004) The factors governing the summer regime of the eastern Mediterranean. Int J Climatol 24:1859–1871